INSTITUTE OF MATHEMATICS

THE CZECH ACADEMY OF SCIENCES

A virtual overlapping Schwarz method for scalar elliptic problems in two dimensions

Juan Gabriel Calvo

Preprint No. 25-2017

PRAHA 2017

A VIRTUAL OVERLAPPING SCHWARZ METHOD FOR SCALAR ELLIPTIC PROBLEMS IN TWO DIMENSIONS

JUAN G. CALVO *

Abstract. A new coarse space for domain decomposition methods is presented for nodal elliptic problems in two dimensions. The coarse space is derived from the novel virtual element methods and therefore can accommodate quite irregular polygonal subdomains. It has the advantage with respect to previous studies that no discrete harmonic extensions are required. The virtual element method allows to handle polygonal meshes and then the algorithm can be used as a preconditioner for linear systems that arise from a discretization with such triangulations. A bound is obtained for the condition number of the preconditioned system by using a two-level overlapping Schwarz algorithm, but the coarse space can be used for different substructuring methods. This bound is independent of jumps in the coefficient across the interface between the subdomains. Numerical experiments that verify the result are shown, including some with triangular, square, hexagonal and irregular elements and with irregular subdomains obtained by a mesh partitioner.

Key words. domain decomposition, overlapping Schwarz algorithms, nodal elliptic problems, irregular subdomain boundaries, virtual element methods

AMS subject classifications. 65F08, 65F10, 65N30, 65N55

1. Introduction. The Virtual Element Methods (VEM) were introduced in [1], while some practical aspects were presented in [2]. As mentioned in [2], some advantages of the VEM are its efficiency and accuracy in computations and its simplicity in implementation. The virtual element space contains a certain number of polynomials to guarantee accuracy, plus additional virtual functions that are never required to be computed. In this way, polygonal elements can be considered for the discretization of partial differential equations. In order to construct a suitable stiffness matrix, a different bilinear form is considered which can be computed by only knowing the degrees of freedom of the virtual functions. We will present the basic theory that corresponds to the lowest-order virtual element functions. In this case, the local virtual space consists of functions that are piecewise-linear and continuous on the boundary and harmonic in the interior of each element.

We will study the scalar elliptic problem in two dimensions

$$-\nabla\cdot(\rho(\boldsymbol{x})\nabla u(\boldsymbol{x}))=f(\boldsymbol{x}),\quad \boldsymbol{x}\in\Omega,\quad \rho(\boldsymbol{x})>0,\quad f\in L^2(\Omega), \tag{1}$$

with homogeneous Dirichlet boundary conditions and posed in the Sobolev space

$$H^1(\Omega):=\{v\in L^2(\Omega):\|\nabla v\|_{L^2(\Omega)}<\infty\}.$$

We will work as usual with a weak formulation for problem (1), namely: Find $u\in H^1_0(\Omega)$ such that

$$a(u,v)=F(v)\quad\forall\ v\in H^1_0(\Omega), \tag{2}$$

where $a(u,v):=\int_\Omega \rho\,\nabla u\cdot\nabla v\,d\boldsymbol{x}$, $F(v):=(f,v)_{0,\Omega}$ is the usual inner product in $L^2(\Omega)$ and $H^1_0(\Omega)$ is the subspace of $H^1(\Omega)$ with zero trace.

For simplicity we will consider a two-level overlapping Schwarz method in this paper, but our new coarse space can also replace the coarse spaces of different iterative

*Institute of Mathematics, Czech Academy of Sciences, Žitná 25, Praha 01, 110 01. (calvo@math.cas.cz). The author gratefully acknowledges the institutional support RVO 67985840.

substructuring algorithms; see [21, Chapter 5]. Two-level overlapping methods were introduced in [13, 14, 15] and a complete theoretical analysis can be found in [21, Chapter 2]. The implementation of our additive preconditioner is straightforward and it only requires the knowledge of the fully assembled matrix, as opposed to non-overlapping methods where the local subdomain matrices are needed.

In order to discretize problem (2) we consider a triangulation $\mathcal{T}_h$ which can be composed by different type of polygons as discussed in Section 2. The domain Ω is then partitioned into N non-overlapping subdomains $\{\Omega_i\}_{i=1}^N$ of diameter H_i which are the union of elements of the triangulation $\mathcal{T}_h$. For the two-level approach, we will consider local problems on extensions $\Omega_i' \supset \Omega_i$ and a coarse problem that involves just a few degrees of freedom related to all the subdomains. In practice, these subdomains can be quite irregular for example if they are obtained from a mesh partitioner, and then there is no straightforward approach to define the coarse basis functions for such subdomains.

If the dimension of the coarse space increases then it can become a bottleneck in a parallel implementation. Therefore it is desirable to have a small coarse space; see [12] for a recent study on small coarse spaces for elliptic problems in three dimensions. For this reason, we will consider two variants: the virtual space on the coarse mesh and a particular subset of this space. Even for structured hexagonal meshes, the reduction in the dimension of the space is quite significant and the estimates for the condition number of the preconditioned system are similar. We construct then the reduced coarse space with just one degree of freedom per subdomain vertex (the nodes of the triangulation that belong to three or more subdomains).

Preconditioning linear systems arising from the discretization of elliptic operators on irregular subdomains has been studied in the past few years. In two dimensions, the issues related to irregular geometry of the subdomains are now better understood. For problems in $H^1(\Omega)$ the first results were established for John [16] and Jones [17] domains in [8, 19, 22, 10]. We note that the coarse spaces considered in these studies are based on energy minimization starting with [9]. The lowest-order virtual element space intrinsically incorporates this condition, since functions are harmonic and therefore have minimum energy. For problems in $H(\mathrm{curl})$, some domain decomposition methods with irregular subdomains are analyzed in [11, 6, 7].

It is also common to have discontinuities in the coefficient ρ, so it is very restrictive to assume that it is constant. Our aim is to develop an algorithm that can be defined for irregular subdomain geometries and that works well even if ρ is not continuous. However, we will assume that ρ is constant on each subdomain Ω_i. For this case, the bounds for the condition number obtained in Theorem 3.1 and Theorem 6.1 are independent of discontinuities of ρ across the interface.

There are two practical approaches for the algorithm presented in this paper. First, for standard discretization methods of problem (2) with linear or bilinear elements, we can use the coarse virtual element space to construct a coarse global component for the preconditioner; see examples in Subsection 7.1. In this way, we can consider quite irregular subdomains in the decomposition. The main advantage of our virtual coarse space with respect to previous studies is that no discrete harmonic extension is required in the algorithm, saving computational time. Second, there is a lack of iterative solvers specifically designed for problems discretized by VEM. We aim to start this analysis by presenting in this paper an estimate for the condition number of the preconditioned system obtained by a two-level overlapping Schwarz algorithm; see examples in Subsection 7.2.

The rest of this paper is organized as follows. In Section 2 we introduce the basic theory of VEM and the discretization of our problem. The two-level overlapping Schwarz method is described in Section 3. Then, in Section 4 we include some technical tools that will be used to obtain the bound of the condition number of the preconditioned system presented in Section 5. In Section 6 we study a variant of the virtual coarse space in order to reduce its dimension significantly. Finally, we report on some numerical experiments in Section 7 and present some final remarks in Section 8.

2. Virtual Element Methods and discretization. In this section we briefly present the Virtual Element Methods. We restrict our presentation to the lowest-order case, but a more general theory is introduced in [1].

Given $h > 0$, we divide the domain Ω into simply connected polygons K (not necessarily similar) of diameter $h_K \leq h$; see some examples in Section 7. We will refer to these polygons as elements and later we will introduce two assumptions on them. This polygonal triangulation will be called *fine mesh* and will be represented by $\mathcal{T}_h$. The *set of nodes* of a partition $\mathcal{T}_h$ contains the vertices of all the elements $K \in \mathcal{T}_h$ and will be denoted by $S_{\mathcal{N}}$, while the set $S_{\mathcal{N}}^K$ includes only the nodes of $\mathcal{T}_h$ that are on the boundary of K. We note that the set $S_{\mathcal{N}}^K$ can contain, besides vertices of K, also hanging nodes, i.e., vertices of other polygons that lie on an edge of K.

We now define for each element K the functions in the virtual element space. Let

$$\mathcal{B}_1(\partial K) := \{v \in C^0(\partial K) : v|_e \in \mathcal{P}_1(e) \quad \forall\, e \subset \partial K\},$$

where e represents any edge on the boundary of K and $\mathcal{P}_1$ is the space of linear polynomials. We consider then the set of lowest-order local virtual element functions, defined by

$$V^K := \{v \in H^1(K) : v \in \mathcal{B}_1(\partial K),\ \Delta v = 0 \text{ in } K\}.$$

Thus, functions are completely determined by their value at the nodes in $S_{\mathcal{N}}^K$ and V^K contains the space of linear polynomials. Then, we define the global space of finite element functions as

$$V_h := \{v \in H_0^1(\Omega) : v|_K \in V^K \ \forall\ K \in \mathcal{T}_h\}.$$

Therefore the dimension of V_h is equal to the number of nodes in the interior of Ω. It is easy to check that they are unisolvent; see, e.g., [1, Proposition 4.1] for a general proof. It is clear that V_h reduces to the first-order Lagrange finite element space in the case of a triangular mesh.

We consider the canonical basis $\{\phi_{\boldsymbol{x}_i}^h\}_{i=1}^{|S_{\mathcal{N}}|}$ for V_h such that for any node $\boldsymbol{x}_j \in S_{\mathcal{N}}$ we have that $\phi_{\boldsymbol{x}_i}^h(\boldsymbol{x}_j) = \delta_{ij}$. For a continuous function u, we define its linear interpolant I^h onto V_h by

$$I^h u := \sum_{\boldsymbol{x}_i \in S_{\mathcal{N}}} u(\boldsymbol{x}_i)\phi_{\boldsymbol{x}_i}^h.$$

In general it is not possible to evaluate $a(\phi_{\boldsymbol{x}_i}^h, \phi_{\boldsymbol{x}_j}^h)$; see the discussion in [1, Section 4.5]. To overcome this issue, a different bilinear form $a_h(\cdot,\cdot)$ satisfying consistency and stability properties is considered. For this purpose we first define a projection onto the space of linear polynomials. Let $a^K(\cdot,\cdot)$ be the bilinear form restricted to the element K, i.e.,

$$a^K(u,v) := \int_K \rho\ \nabla u \cdot \nabla v\ d\boldsymbol{x}.$$

Define the operator $\widehat{\Pi}^K : V^K \to \mathcal{P}_1(K) \subset V^K$ where $\widetilde{v} := \widehat{\Pi}^K v \in \mathcal{P}_1(K)$ is the linear polynomial that satisfies

$$\begin{cases} a^K(\widetilde{v}, q) = a^K(v, q) \quad \forall\, q \in \mathcal{P}_1(K), \\ \overline{\widetilde{v}} = \overline{v}, \end{cases}$$

where $\overline{w}$ denotes the standard nodal average of w,

$$\overline{w} := \frac{1}{|S_{\mathcal{N}}^K|} \sum_{\boldsymbol{x} \in S_{\mathcal{N}}^K} w(\boldsymbol{x}).$$

From the definition it is clear that $\widehat{\Pi}^K v = v$ for $v \in \mathcal{P}_1(K)$. Given $q \in \mathcal{P}_1(K)$ and $v \in V^K$, $a^K(v, q)$ is computed from Green's identity

$$a^K(v, q) = \int_K \nabla v \cdot \nabla q \; d\boldsymbol{x} \; = \int_{\partial K} v \; \frac{\partial q}{\partial \boldsymbol{n}} \; d\boldsymbol{s},$$

since $\Delta q = 0$. The last integral can be computed exactly by just knowing the degrees of freedom of v; see [2] for implementation details.

The discrete local bilinear form $a_h^K : V^K \times V^K \to \mathbb{R}$ is then defined by

$$a_h^K(u, v) := a^K(\widehat{\Pi}^K u, \widehat{\Pi}^K v) + S^K(u - \widehat{\Pi}^K u, v - \widehat{\Pi}^K v), \tag{3}$$

where $S^K : V^K \times V^K \to \mathbb{R}$ is a stabilizing term, which can be chosen as

$$S^K(u, v) := \sum_{\boldsymbol{x} \in S_{\mathcal{N}}^K} \rho \; u(\boldsymbol{x}) v(\boldsymbol{x}).$$

We consider the following two assumptions where h denotes the maximum of the diameters of the elements in $\mathcal{T}_h$:

Assumption 1. *There exists $\gamma > 0$ such that for all h, each element K in $\mathcal{T}_h$ is star-shaped with respect to a ball of radius greater than or equal to γh_K.*

Assumption 2. *There exists $\gamma > 0$ such that for all h and for each element K in $\mathcal{T}_h$, the distance between any two vertices of K is greater than or equal to γh_K.*

Remark 2.1. Assumption 1 ensures the existence of a local polynomial with optimal approximation properties; see [1, Propositions 4.2, 4.3]. As mentioned in [1, Remark 4.3], we could take the weaker assumption that every K is the union of a uniformly bounded number of star-shaped domains, each satisfying Assumption 1. In turn, Assumption 2 guarantees the stability of the bilinear form; see (4) below.

Remark 2.2. As mentioned in [1, Section 4.6], in their numerical experiments the method appears to be quite robust with respect to Assumption 2. We also have not found any difficulty when considering elements where the lengths of its sides have different orders of magnitude; see Subsection 7.2 for experiments with irregular polygons.

From (3) it is clear that a_h^K satisfies the consistency property

$$a_h^K(p, v) = a^K(p, v) \quad \forall\, p \in \mathcal{P}_1(K), \quad \forall\, v \in V^K.$$

The stability property

$$\alpha_1 a^K(v, v) \le a_h^K(v, v) \le \alpha_2 a^K(v, v) \quad \forall\, v \in V^K \tag{4}$$

follows from [1, Theorem 4.1], where α_1, α_2 are independent of K, h_K and ρ. The discrete bilinear form and right-hand side are then defined by

$$a_h(u,v) := \sum_{K\in\mathcal{T}_h} a_h^K(u,v), \quad F_h(v) := \sum_{K\in\mathcal{T}_h} \int_K \mathbb{P}_0^K(f)\ \overline{v}\ d\boldsymbol{x},$$

respectively. Here, $\mathbb{P}_0^K$ is the L^2-projection onto the space of constants; see [1, Section 4.7]. Finally, our discrete formulation for problem (2) is: Find $u_h \in V_h$ such that

$$a_h(u_h, v_h) = F_h(v_h) \quad \forall\ v_h \in V_h. \tag{5}$$

We refer to [1, 5] for an a priori estimate and approximation properties.

3. Overlapping Schwarz methods. We briefly describe the two-level additive overlapping Schwarz methods; for a complete study see [21, Chapters 2, 3]. The need of a coarse level arises from the fact that the condition number estimate deteriorates for any one-level algorithm as the number of subdomain increases.

3.1. The coarse space. The domain Ω is partitioned into N non-overlapping and simply connected subdomains $\{\Omega_i\}_{i=1}^N$ of diameter H_i which are the union of elements of the triangulation $\mathcal{T}_h$; see some examples in Section 7. The partition $\{\Omega_i\}$ will be called *coarse mesh* and will be denoted by $\mathcal{T}_H$. The set of nodes of $\mathcal{T}_H$ contains the vertices of all the subdomains Ω_i and will be represented by $S_{\mathcal{N}}^H$, and the set $S_{\mathcal{N}}^{\Omega_i}$ includes only the nodes of $\mathcal{T}_H$ that are on the boundary of $\partial\Omega_i$. We assume that $\rho(\boldsymbol{x})$ is constant and equal to ρ_i inside each subdomain Ω_i.

The coarse virtual space in $\mathcal{T}_H$ is given by

$$V_0 := \left\{ v \in H_0^1(\Omega) : v|_{\Omega_i} \in \mathcal{B}_1(\partial\Omega_i),\ \Delta v|_{\Omega_i} = 0 \text{ in } \Omega_i, 1 \le i \le N \right\}$$

and the degrees of freedom are the values at the nodes of $\mathcal{T}_H$. For any node $\boldsymbol{x} \in S_{\mathcal{N}}^H$, we denote by $\phi_{\boldsymbol{x}}^H$ the canonical basis function of V_0 that vanishes at all coarse nodes, except at $\boldsymbol{x}$ where it takes the value 1. We can define the linear operator $I^H : V_h \to V_0$ by

$$I^H(u) := \sum_{\boldsymbol{x}\in S_{\mathcal{N}}^H} u(\boldsymbol{x})\phi_{\boldsymbol{x}}^H.$$

In general we cannot compute exactly the values of $I^H u$ at the internal nodes of a subdomain Ω_i. In order to define an operator $R_0^T : V_0 \to V_h$ we could consider the discrete harmonic extension for each subdomain Ω_i by using the bilinear form $a(\cdot,\cdot)$ restricted to Ω_i. Instead, we assemble R_0^T subdomain by subdomain by constructing a triangulation $\mathcal{T}_{\Omega_i}$ of the subdomain Ω_i. For our analysis in Section 4 and Section 5, we will consider $\mathcal{T}_{\Omega_i}$ as an arbitrary (but fixed) triangulation of the nodes in $S_{\mathcal{N}}^{\Omega_i}$.

Given $u_0 \in V_0$ we set $R_0^T u_0(\boldsymbol{x}) := u_0(\boldsymbol{x})$ for the coarse nodes $\boldsymbol{x} \in S_{\mathcal{N}}^{\Omega_i}$. We then compute the degrees of freedom of $R_0^T u_0 \in V_h$ by evaluating the piecewise-linear interpolant onto $\mathcal{T}_{\Omega_i}$. Hence, no discrete harmonic extensions are required in order to construct R_0^T in contrast to previous coarse spaces; see, e.g., [10]. Even though, our theoretical bound for the condition number and the numerical results are quite similar as theirs.

Finally, we consider the bilinear form defined in $V_0 \times V_0$ by

$$\tilde{a}_{h,0}(u_0, v_0) := a_h(R_0^T u_0, R_0^T v_0) = \sum_{K\in\mathcal{T}_h} a_h^K(R_0^T u_0, R_0^T v_0). \tag{6}$$

3.2. Local spaces. We now construct overlapping subdomains $\Omega_i' \supset \Omega_i$ by adding layers of elements that are external to Ω_i, and we denote by δ_i the width of the region $\Omega_i' \setminus \Omega_i$. We then consider the local virtual spaces V_i, $1 \leq i \leq N$, defined by

$$V_i := \left\{ v \in H_0^1(\Omega_i') : v|_K \in \mathcal{B}_1(\partial K),\ \Delta v|_K = 0 \text{ in } K,\ \forall\, K \subset \Omega_i' \right\}.$$

Thus, the degrees of freedom are the values at the nodes of $\mathcal{T}_h$ in the interior of Ω_i'. We also consider the natural operators $R_i^T : V_i \to V_h$ given by the zero extension from the subdomain Ω_i' to Ω, $1 \leq i \leq N$. We use exact solvers for the local spaces, i.e., we define the bilinear forms $\tilde{a}_{h,i} : V_i \times V_i \to \mathbb{R}$ given by

$$\tilde{a}_{h,i}(u_i, v_i) := a_h(R_i^T u_i, R_i^T v_i) = \sum_{K \subset \Omega_i'} a_h^K(u_i, v_i), \tag{7}$$

for $1 \leq i \leq N$; see [21, Chapter 2].

3.3. Algorithm. The discrete problem (5) can be written as the ill-conditioned sparse linear system

$$A\boldsymbol{\lambda} = \boldsymbol{g},$$

where $A_{i,j} = a_h(\phi_{\boldsymbol{x}_j}^h, \phi_{\boldsymbol{x}_i}^h)$, $\boldsymbol{g}_i = F_h(\phi_{\boldsymbol{x}_i}^h)$ and $\boldsymbol{\lambda}$ is the vector of coordinates of the solution with respect to the basis $\{\phi_{\boldsymbol{x}_i}^h\}$ of V_h, i.e., $u_h = \sum \lambda_i \phi_{\boldsymbol{x}_i}^h$. In this subsection we present a scalable preconditioner for this linear system which allows for parallel implementation.

Consider the matrix representation of the operators R_i^T denoted again by R_i^T. We define the stiffness matrices $\tilde{A}_i = R_i A R_i^T$, $0 \leq i \leq N$, and then consider the Schwarz projections

$$P_i = R_i^T \tilde{A}_i^{-1} R_i A,\ 0 \leq i \leq N.$$

The additive preconditioned operator is defined by

$$P_{ad} := \sum_{i=0}^{N} P_i = A_{ad}^{-1} A, \text{ with } A_{ad}^{-1} = \sum_{i=0}^{N} R_i^T \tilde{A}_i^{-1} R_i. \tag{8}$$

Multiplicative and hybrid preconditioners can be considered as well; see [21, Section 2.2]. For the preconditioned system $A_{ad}^{-1} A\boldsymbol{\lambda} = A_{ad}^{-1}\boldsymbol{g}$, we have the main theorem of this paper. Its proof is presented in Section 5.

THEOREM 3.1. *There exists a constant C, independent of H, h and ρ, such that the condition number of the preconditioned system $\kappa(A_{ad}^{-1}A)$ satisfies*

$$\kappa(A_{ad}^{-1}A) \leq C \left(1 + \log \frac{H}{h}\right) \left(1 + \frac{H}{\delta}\right),$$

where the ratios H/h and H/δ denote their maximum value over all the subdomains.

4. Technical Tools. We collect some tools that will be needed in Section 5. We start with the following Poincaré inequality and discrete Sobolev inequality:

LEMMA 4.1. *Let Ω be Lipschitz continuous with diameter H. Then, there exists a constant C that depends only on the shape of Ω but not on H, such that*

$$\|v\|_{L^2(\Omega)}^2 \leq C H^2 |v|_{H^1(\Omega)}^2,$$

for $v \in H^1(\Omega)$ with vanishing mean value $\widehat{v} := \dfrac{1}{|\Omega|}\displaystyle\int_\Omega v \, d\boldsymbol{x}$.

Proof. See [21, Corollary A.15]. ∎

LEMMA 4.2. *There exists a constant C, independent of H_i and h_i, such that*

$$\|v\|^2_{L^\infty(\Omega_i)} \leq C\left(1+\log\frac{H_i}{h_i}\right)\|v\|^2_{H^1(\Omega_i)}, \quad \text{for } v \in V_h.$$

In particular, if u has zero mean value, then

$$\|v\|^2_{L^\infty(\Omega_i)} \leq C\left(1+\log\frac{H_i}{h_i}\right)|v|^2_{H^1(\Omega_i)}.$$

Proof. See [3], [4, Section 4.9] for a proof with domains satisfying an interior cone condition. This inequality holds for more general subdomains; see, e.g., [8, Lemma 3.2] for a proof with John domains. The second inequality is a consequence of Lemma 4.1. ∎

We now obtain some bounds for the operators introduced in Subsection 3.1:

LEMMA 4.3. *Given $u \in V_h$, let $u_0 := I^H u \in V_0$. Then, there exists a constant C such that*

$$\|u - R_0^T u_0\|^2_{L^2(\Omega_i)} \leq C H_i^2\left(1+\log\frac{H_i}{h_i}\right)|u|^2_{H^1(\Omega_i)},$$

where C is independent of H_i and h_i.

Proof. Let $\widehat{u}$ be the mean value of u over Ω_i. By triangle inequality and Lemma 4.1, we have that

$$\begin{aligned}\|u - R_0^T u_0\|^2_{L^2(\Omega_i)} &\leq 2\left(\|u-\widehat{u}\|^2_{L^2(\Omega_i)} + \|R_0^T u_0 - \widehat{u}\|^2_{L^2(\Omega_i)}\right)\\ &\leq C H_i^2\left(|u|^2_{H^1(\Omega)} + \|R_0^T(u_0-\widehat{u})\|^2_{L^\infty(\Omega_i)}\right)\end{aligned}$$

since R_0^T reproduces constants. From the definition of the operator R_0^T, it holds that

$$\|R_0^T(u_0-\widehat{u})\|_{L^\infty(\Omega_i)} = \|I^H(u-\widehat{u})\|^2_{L^\infty(\Omega_i)} \leq \|u-\widehat{u}\|^2_{L^\infty(\Omega_i)}.$$

We conclude our proof by using Lemma 4.2. ∎

LEMMA 4.4. *Given $u \in V_h$, let $u_0 := I^H u \in V_0$. Then, there exists a constant C such that*

$$|u_0|^2_{H^1(\Omega_i)} \leq |R_0^T u_0|^2_{H^1(\Omega_i)} \leq C\left(1+\log\frac{H_i}{h_i}\right)|u|^2_{H^1(\Omega_i)},$$

where C is independent of H_i and h_i.

Proof. The first inequality follows from the fact that u_0 and $R_0^T u_0$ have the same boundary data on $\partial\Omega_i$, and $u_0 \in V_0$ has minimum energy. Next, consider a fixed triangulation $\mathcal{T}_{\Omega_i}$ of the nodes in $S_{\mathcal{N}}^{\Omega_i}$ and denote by I_T the nodal interpolant onto $\mathcal{T}_{\Omega_i}$. Furthermore, for any element $K \subset \Omega_i$, let $\mathcal{T}_K$ be a triangular partition of K and define I_K as the nodal interpolant onto $\mathcal{T}_K$; see Figure 1. For simplicity we write $u_h := R_0^T u_0$.

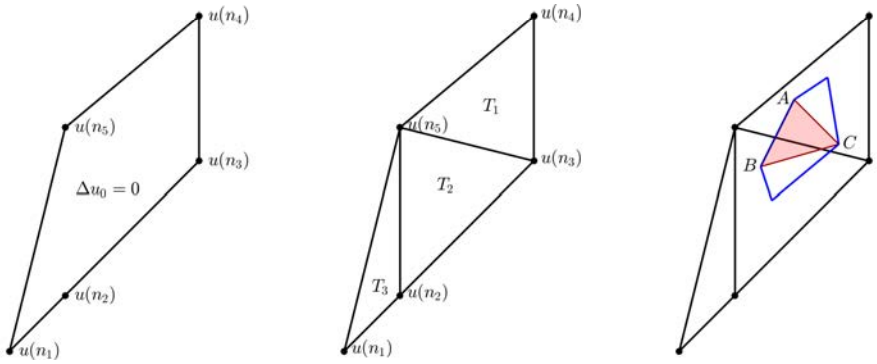

Fig. 1: Geometry in the proof of Lemma 4.4: (a) A subdomain Ω_i with five edges; the degrees of freedom for u_0 are the values of u at the nodes $n_j \in S_{\mathcal{N}}^{\Omega_i}$ (left). (b) Triangulation $\mathcal{T}_{\Omega_i} = \{T_1, T_2, T_3\}$ for Ω_i; I_T is obtained from the nodal values of u (middle). (c) An element K (in blue) and its triangulation $\mathcal{T}_K$ where $\triangle ABC$ intersects T_1 and T_2 (right).

We have that

$$|u_h|^2_{H^1(K)} \leq |I_K u_h|^2_{H^1(K)} = \sum_{T_K \in \mathcal{T}_K} |I_K u_h|^2_{H^1(T_K)}$$

since $u_h = I_K u_h$ on ∂K. We claim that

$$|I_K u_h|_{H^1(T_K)} \leq |I_T u|_{H^1(\omega_{T_K})} \quad \forall\, T_K \in \mathcal{T}_K, \tag{9}$$

where ω_{T_K} is the union of T_K and its neighboring triangles (that are in $\mathcal{T}_{\widetilde{K}}$ for some $\widetilde{K} \subset \Omega_i$). If T_K lies inside a triangle $T \in \mathcal{T}_{\Omega_i}$, then $u_h|_{T_K}$ is a linear polynomial and $|I_K u_h|_{H^1(T_K)} = |I_T u|_{H^1(T_K)}$. Thus, we need to study only the case when T_K intersects at least two triangles $T_1, T_2 \in \mathcal{T}_{\Omega_i}$. Let T_K be one of such triangles with vertices A, B, C as in Figure 1. Then,

$$|I_K u_h|^2_{H^1(T_K)} \leq C \left(|I_T u(A)|^2 + |I_T u(B)|^2 + |I_T u(C)|^2 \right),$$

since the energy of the basis functions are uniformly bounded by Assumption 2. We now bound the three terms on the right hand side separately. Following similar ideas as in [21, Lemma 3.8], we can find a shape-regular triangle $\widetilde{T} \subset \omega_{T_K}$ with vertices A, B', C' and diameter of order h_K which is a subset of a triangle $T \in \mathcal{T}_{\Omega_i}$. Then,

$$|I_T u(A)|^2 \leq |I_T u(A)|^2 + |I_T u(B')|^2 + |I_T u(C')|^2 \leq C h_K^{-2} \|I_T u\|^2_{L^2(\widetilde{T})}.$$

We bound the other two terms similarly to obtain

$$|I_K u_h|^2_{H^1(T_K)} \leq C h_K^{-2} \|I_T u\|^2_{L^2(\omega_{T_K})}.$$

If we replace u by $u - c$, the left-hand side does not change since I^H and R_0^T reproduce constants. We can use then Lemma 4.1 to bound the right-hand side by choosing c as the mean value of $I_T u$ on ω_{T_K}. Hence, Equation (9) holds and then

$$|u_h|^2_{H^1(\Omega_i)} \leq C |I_T u|^2_{H^1(\Omega_i)}.$$

Finally, for any $T \in \mathcal{T}_{\Omega_i}$ we have that

$$|I_T u|^2_{H^1(T)} = |I_T(u - \widehat{u}_T)|^2_{H^1(T)} \leq C\|u - \widehat{u}_T\|^2_{L^\infty(T)} \leq C\left(1 + \log\frac{H_i}{h_i}\right)|u|^2_{H^1(T)},$$

where we have used Lemma 4.2. We conclude our proof by adding the contributions from all $T \in \mathcal{T}_{\Omega_i}$. ∎

We need also a partition of unity in order to obtain local functions that will be components of our stable decomposition:

LEMMA 4.5. *There exists a family of functions* $\{\tilde{\theta}_i\}_{i=1}^N$ *in* $W^{1,\infty}(\Omega)$ *such that* $0 \leq \tilde{\theta}_i(x) \leq 1$, $\sum_i \tilde{\theta}_i(x) = 1$ *for* $x \in \overline{\Omega}$, $supp(\tilde{\theta}_i) \subset \overline{\Omega_i'}$ *and*

$$\|\nabla\tilde{\theta}_i\|_{L^\infty(\Omega_i')} \leq C/\delta_i,$$

where C *is independent of* δ_i *and* H_i.

Proof. See [21, Lemma 3.4]. ∎

We conclude this section with the following lemma:

LEMMA 4.6. *Let* $K \in \mathcal{T}_h$ *and consider any triangular partition* $\mathcal{T}_K$ *of* K. *Suppose that* $u \in H^1(\Omega)$ *is a quadratic function in each triangle* $T \in \mathcal{T}_K$. *Then, there exists a constant* C, *independent of* h_K, *such that*

$$|I^h u|_{H^1(K)} \leq C|u|_{H^1(K)}.$$

Proof. This is a modification of [21, Lemma 3.9]. Denote by I_K the nodal piecewise-linear interpolant onto $\mathcal{T}_K$. Since $I^h u$ has minimum energy, it holds that

$$\begin{aligned}|I^h u|^2_{H^1(K)} \leq |I_K u|^2_{H^1(K)} &= \sum_{T\in\mathcal{T}_K} |I_K u|^2_{H^1(T)} \\ &\leq 2|u|^2_{H^1(K)} + 2\sum_{T\in\mathcal{T}_K} |I_K u - u|^2_{H^1(T)}.\end{aligned}$$

By using a standard error bound and an elementary inverse inequality as in [21, Lemma 3.9], it follows that

$$|I_K u - u|^2_{H^1(T)} \leq C H_T^2 |u|^2_{H^2(T)} \leq C|u|^2_{H^1(T)},$$

where H_T is the diameter of T. We conclude the proof by combining the last two inequalities. ∎

5. Condition number. We follow the theory developed in [21, Chapter 2] in order to estimate $\kappa(P_{ad})$. The condition number of the additive operator (8) is bounded by

$$\kappa(P_{ad}) \leq (N^C + 1)C_0^2,$$

where N^C is the minimum number of colors needed to color the overlapping subdomains Ω_i' such that no pair of subdomains of the same color intersect, and C_0 is a constant such that

$$\sum_{i=0}^N \tilde{a}_{h,i}(u_i, u_i) \leq C_0^2\ a_h(u,u), \quad \text{where} \quad u = \sum_{i=0}^N R_i^T u_i, u_i \in V_i;$$

see [21, Theorem 3.13]. Clearly, as the overlap increases, the number of colors required might increase while C_0 will decrease. We now present the proof of Theorem 3.1:

Proof. (Theorem 3.1) For simplicity we write $\omega_i := 1 + \log(H_i/h_i)$ and let $\omega := \max_i \omega_i$. We first define $u_0 := I^H u \in V_0$. From (6), (4) and Lemma 4.4 it holds that

$$\begin{aligned}\tilde{a}_{h,0}(u_0,u_0) &\leq \alpha_2 \sum_{i=1}^{N} a^{\Omega_i}(R_0^T u_0, R_0^T u_0) \leq C\alpha_2 \sum_{i=1}^{N} \omega_i a^{\Omega_i}(u,u) \\ &\leq C\frac{\alpha_2}{\alpha_1}\omega \sum_{K\in\mathcal{T}_h} a_h^K(u,u) = C\frac{\alpha_2}{\alpha_1}\omega a_h(u,u). \end{aligned} \tag{10}$$

Define $w := u - R_0^T u_0$ and let $u_i := R_i(I^h(\tilde{\theta}_i w)) \in V_i$ with $\tilde{\theta}_i$ as in Lemma 4.5. We have that

$$R_0^T u_0 + \sum_{i=1}^{N} R_i^T u_i = R_0^T u_0 + \sum_{i=1}^{N} I^h(\tilde{\theta}_i w) = R_0^T u_0 + I^h\left(\sum_{i=1}^{N} \tilde{\theta}_i w\right) = u$$

since $I^h v = v$ for $v \in V_h$. From (7) and (4) we have that

$$\tilde{a}_{h,i}(u_i,u_i) \leq \alpha_2 \sum_{K\subset\Omega_i'} a^K(u_i,u_i) = \alpha_2 \sum_{K\subset\Omega_i'} \int_K \rho|\nabla(I^h(\tilde{\theta}_i w))|^2 \, d\boldsymbol{x}. \tag{11}$$

For any element $K \in \mathcal{T}_h$, we consider an arbitrary (but fixed) triangular mesh $\mathcal{T}_K$ of K, and denote by I_K the piecewise-linear interpolant onto $\mathcal{T}_K$. Define the piecewise-linear functions θ_i^ℓ and w^ℓ element by element by

$$\theta_i^\ell|_K := I_K\tilde{\theta}_i \text{ and } \; w^\ell|_K := I_K w.$$

It is clear that in this way θ_i^ℓ satisfies the same properties of Lemma 4.5, since $\|\nabla\theta_i^\ell\|_{L^\infty(K)} \leq \|\nabla\tilde{\theta}_i\|_{L^\infty(K)}$.

By using Lemma 4.6, we deduce that

$$|I^h(\tilde{\theta}_i w)|^2_{H^1(K)} = |I^h(\theta_i^\ell w^\ell)|^2_{H^1(K)} \leq C|\theta_i^\ell w^\ell|^2_{H^1(K)}$$

and substituting in (11) yields to

$$\tilde{a}_{h,i}(u_i,u_i) \leq C\alpha_2 \left(\int_{\Omega_i'} \rho|\theta_i^\ell \nabla w^\ell|^2 \, d\boldsymbol{x} + \int_{\Omega_i'} \rho|w^\ell \nabla\theta_i^\ell|^2 \, d\boldsymbol{x}\right). \tag{12}$$

It holds that

$$|w^\ell|^2_{H^1(K)} \leq Ch_K^2\|\nabla w^\ell\|^2_{L^\infty(K)} \leq Ch_K^2\|\nabla w\|^2_{L^\infty(K)} \leq C\|w\|^2_{H^1(K)} \tag{13}$$

where we have used an inverse inequality in the last step; see, e.g., [4, Lemma 4.5.3]. Since $|\theta_i^\ell| \leq 1$, the first term in the sum of (12) can be bounded easily by

$$\begin{aligned}\int_{\Omega_i'} \rho \, |\theta_i^\ell \nabla w^\ell|^2 \, d\boldsymbol{x} &\leq C \sum_{j\in\Xi_i} \rho_j \|w\|^2_{H^1(\Omega_j)} \\ &= C \sum_{j\in\Xi_i} \rho_j \left(H_j^{-2}\|u - R_0^T u_0\|^2_{L^2(\Omega_j)} + |u - R_0^T u_0|^2_{H^1(\Omega_j)}\right) \\ &\leq C\omega \sum_{j\in\Xi_i} \rho_j |u|^2_{H^1(\Omega_j)} = C\omega \sum_{j\in\Xi_i} a^{\Omega_j}(u,u), \end{aligned} \tag{14}$$

where we have used triangle inequality, Lemma 4.3 and Lemma 4.4. Here, $\Xi_i := \{j : \overline{\Omega}_j \cap \overline{\Omega}_i \neq \emptyset\}$.

In order to estimate the last term in (12), the gradient of θ_i^ℓ is not zero only in a neighborhood of $\partial\Omega_i$ of width $\max_{j\in\Xi_i} \delta_j$. The number of sets Ω'_j that intersect Ω_i is uniformly bounded, and therefore we need to consider the contribution from only one of them. We write $w^\ell = w_1^\ell + w_2^\ell$, with $w_1^\ell|_K := I_K(u - u_0)$ and $w_2^\ell|_K := I_K(u_0 - R_0^T u_0)$ for each element K.

We first note that

$$\|w_1^\ell\|_{L^\infty(\Omega_i)} \leq \|u - \widehat{u}\|_{L^\infty(\Omega_i)} + \|I^H(u - \widehat{u})\|_{L^\infty(\Omega_i)} \leq 2\|u - \widehat{u}\|_{L^\infty(\Omega_i)},$$

where $\widehat{u}$ is the mean average of u over Ω_i.

Therefore,

$$\int_{\Omega'_j\cap\Omega_i} \rho_i \, |w_1^\ell \nabla\theta_i^\ell|^2 \, d\boldsymbol{x} \leq C \, \frac{\rho_i}{\delta_i^2} \, \|u - \widehat{u}\|^2_{L^\infty(\Omega_i)} |\Omega'_j \cap \Omega_i| \leq C \, \frac{H_i}{\delta_i} \, \omega_i a^{\Omega_i}(u,u). \tag{15}$$

For the remaining term w_2^ℓ, we cover $\Omega'_j \cap \Omega_i$ with square patches with sides on the order of δ_i and note that on the order of H_i/δ_i of them will suffice. For a square π_k we can bound

$$\int_{\pi_k} \rho_i |w_2^\ell \nabla\theta_i^\ell|^2 \, d\boldsymbol{x} \leq \frac{C}{\delta_i^2} \rho_i \, \|w_2^\ell\|^2_{L^2(\pi_k)} \leq C\rho_i |w_2^\ell|^2_{H^1(\pi_k)}$$

where we have used a Friedrich's inequality, since w_2^ℓ vanishes on $\partial\Omega_i$. By adding all the contributions from the squares π_k we get

$$\begin{aligned} \int_{\Omega'_j\cap\Omega_i} \rho_i |w_2^\ell \nabla\theta_i^\ell|^2 \, d\boldsymbol{x} &\leq C\rho_i |w_2^\ell|^2_{H^1(\Omega_i)} \leq C\rho_i \|u_0 - R_0^T u_0\|^2_{H^1(\Omega_i)} \\ &\leq C\rho_i |u_0 - R_0^T u_0|^2_{H^1(\Omega_i)} \leq C\rho_i w_i |u|^2_{H^1(\Omega_i)}, \end{aligned} \tag{16}$$

where we have used a similar argument as in (13), the fact that $u_0 - R_0^T u_0$ vanishes on $\partial\Omega_i$, and Lemma 4.4. From (15) and (16) we obtain that

$$\int_{\Omega'_j\cap\Omega_i} \rho_i |w^\ell \nabla\theta_i^\ell|^2 \, d\boldsymbol{x} \leq C \, \left(1 + \frac{H_i}{\delta_i}\right) \, \omega_i a^{\Omega_i}(u,u),$$

and by adding all the contributions of the sets $\Omega'_j \cap \Omega_i$ and $\Omega'_i \cap \Omega_j$, we get

$$\int_{\Omega'_i} \rho |w^\ell \nabla\theta_i^\ell|^2 \, d\boldsymbol{x} \leq C \, \left(1 + \frac{H}{\delta}\right) \, \omega \sum_{j\in\Xi_i} a^{\Omega_j}(u,u). \tag{17}$$

Thus, by substituting (14) and (17) in (12), we obtain

$$\begin{aligned} \tilde{a}_{h,i}(u_i,u_i) &\leq C\alpha_2 \, \omega \left(1 + \frac{H}{\delta}\right) \sum_{j\in\Xi_i} \sum_{K\subset\Omega_j} a^K(u,u) \\ &\leq C\frac{\alpha_2}{\alpha_1} \, \omega \left(1 + \frac{H}{\delta}\right) \sum_{j\in\Xi_i} \sum_{K\subset\Omega_j} a_h^K(u,u). \end{aligned} \tag{18}$$

We sum all the contributions from $\tilde{a}_{h,i}(u_i, u_i)$, $i = 0, \ldots, N$. By (10) and (18) we conclude that $\sum_{i=0}^{N} \tilde{a}_{h,i}(u_i, u_i) \leq C_0^2 a_h(u, u)$, with

$$C_0^2 := C\frac{\alpha_2}{\alpha_1}\left(1 + \frac{H}{\delta}\right)\left(1 + \log\frac{H}{h}\right),$$

and our theorem holds. ∎

6. Reduced coarse space. In general it is desirable to have a small coarse space. In our case, the number of vertices of the polygons Ω_i could be quite large even if we have a structured mesh; see for example Table 1 where we report the dimension of the coarse space V_0 when using METIS subdomains. We will introduce a smaller coarse space V_0^R by considering a particular subset of V_0.

Given a decomposition $\{\Omega_i\}_{i=1}^N$ of Ω, we partition the nodes of the triangulation $\mathcal{T}_h$ into equivalence classes. The nodes that belong to exactly one subdomain Ω_i are its *interior nodes*. A *subdomain edge* $\mathcal{E}^{ij}$ will be the interior of the intersection of the closure of two neighboring subdomains Ω_i and Ω_j. If such intersection has more than one component, each open component will be considered as a subdomain edge. Then, the endpoint nodes of $\mathcal{E}^{ij}$ will belong to the set of *subdomain vertices*. We will write $\mathcal{E}$ instead of $\mathcal{E}^{ij}$ if there is no need to identify the two subdomains Ω_i and Ω_j.

Inspired by [10], for each subdomain vertex $\boldsymbol{x}_0$ we will define a coarse function $\psi_{\boldsymbol{x}_0} \in V_0$. First, we set $\psi_{\boldsymbol{x}_0}(\boldsymbol{x}) = 0$ for all subdomain vertices, except at $\boldsymbol{x}_0$ where $\psi_{\boldsymbol{x}_0}(\boldsymbol{x}_0) = 1$. We then define the coarse degrees of freedom for the nodes in the interior of the subdomain edges. If $\boldsymbol{x}_0$ is not an endpoint of $\mathcal{E}$, then $\psi_{\boldsymbol{x}_0}$ vanishes on that edge. If $\mathcal{E}$ has endpoints $\boldsymbol{x}_0$ and $\boldsymbol{x}_1$, let $\boldsymbol{d}_{\mathcal{E}}$ be the unit vector with direction from $\boldsymbol{x}_1$ to $\boldsymbol{x}_0$. Consider any node $\widetilde{\boldsymbol{x}} \in \mathcal{E}$. If $0 \leq (\widetilde{\boldsymbol{x}} - \boldsymbol{x}_1) \cdot \boldsymbol{d}_{\mathcal{E}} \leq |\boldsymbol{x}_0 - \boldsymbol{x}_1|$, we then set

$$\psi_{\boldsymbol{x}_0}(\widetilde{\boldsymbol{x}}) = \frac{(\widetilde{\boldsymbol{x}} - \boldsymbol{x}_1) \cdot \boldsymbol{d}_{\mathcal{E}}}{|\boldsymbol{x}_0 - \boldsymbol{x}_1|}. \tag{19}$$

It is clear that $\psi_{\boldsymbol{x}_0}(\boldsymbol{x}_0) = 1$, $\psi_{\boldsymbol{x}_0}(\boldsymbol{x}_1) = 0$ and that the function varies linearly in the direction of $\boldsymbol{d}_{\mathcal{E}}$ for such nodes. If $(\widetilde{\boldsymbol{x}} - \boldsymbol{x}_1) \cdot \boldsymbol{d}_{\mathcal{E}} < 0$ or $(\widetilde{\boldsymbol{x}} - \boldsymbol{x}_1) \cdot \boldsymbol{d}_{\mathcal{E}} > |\boldsymbol{x}_0 - \boldsymbol{x}_1|$, we then set $\psi_{\boldsymbol{x}_0}(\widetilde{\boldsymbol{x}}) = 0$ or $\psi_{\boldsymbol{x}_0}(\widetilde{\boldsymbol{x}}) = 1$, respectively. In this way, we define all the degrees of freedom of $\psi_{\boldsymbol{x}_0} \in V_0$. By construction it is clear that $\psi_{\boldsymbol{x}_0} \in V_0$ is uniformly bounded and that $\psi_{\boldsymbol{x}_0} + \psi_{\boldsymbol{x}_1} \equiv 1$ along the edge $\mathcal{E}$. We present $R_0^T \psi_{\boldsymbol{x}_0}$ for a particular subdomain vertex in Figure 2, where we have used hexagonal elements and METIS subdomains. We then define the *reduced* coarse space

$$V_0^R := \left\{ v \in H_0^1(\Omega) : v = \sum_{\boldsymbol{x}_0} \alpha_{\boldsymbol{x}_0} \psi_{\boldsymbol{x}_0} \right\} \subset V_0,$$

where the sum goes over all the subdomain vertices $\boldsymbol{x}_0$. In this setting we have only one coarse degree of freedom per subdomain vertex. In the numerical experiments, the dimension of V_0^R is in average just a 6% of the dimension of V_0 for hexagonal and irregular elements. We conclude with an analogous result as Theorem 3.1 for this reduced coarse space:

THEOREM 6.1. *Consider the preconditioner A_{ad}^{-1} obtained by using the reduced coarse space V_0^R. Then, there exists a constant C, independent of H, h and ρ, such that the condition number of the preconditioned system $\kappa(A_{ad}^{-1}A)$ satisfies*

$$\kappa(A_{ad}^{-1}A) \leq C\left(1 + \log\frac{H}{h}\right)\left(1 + \frac{H}{\delta}\right),$$

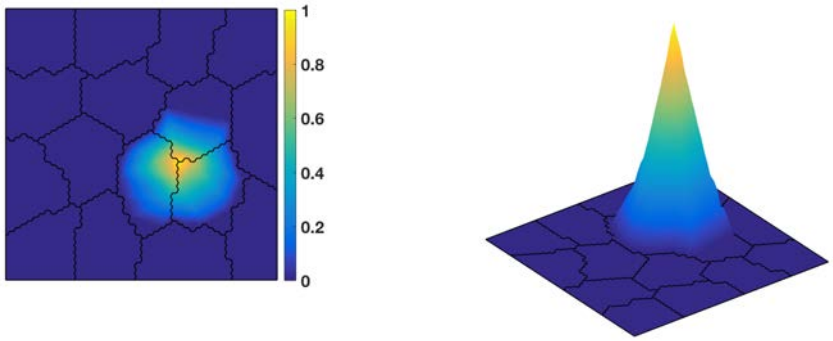

Fig. 2: A reduced coarse basis function for an hexagonal mesh with METIS subdomains.

where the ratios H/h and H/δ denote their maximum value over all the subdomains.

Proof. Given $u \in V_h$ we define $I^{\widetilde{H}}u := \sum_{\boldsymbol{x}_0} u(\boldsymbol{x}_0)\psi_{\boldsymbol{x}_0} \in V_0^R$. We have that $I^{\widetilde{H}}$ reproduces constants and since $V_0^R \subset V_0$, we can write $u_0 := I^{\widetilde{H}}u$ as a linear combination of the coarse basis functions $\phi_{\boldsymbol{x}}^H$ of V_0, where all the degrees of freedom can be expressed in terms of u. More precisely,

$$u_0 = \sum_{\boldsymbol{x}\in S_{\mathcal{V}}} u(\boldsymbol{x})\phi_{\boldsymbol{x}}^H + \sum_{\mathcal{E}}\sum_{\boldsymbol{x}\in\mathcal{E}} \left(\psi_{\boldsymbol{x}_0}(\boldsymbol{x})u(\boldsymbol{x}_0) + (1-\psi_{\boldsymbol{x}_0}(\boldsymbol{x}))u(\boldsymbol{x}_1)\right)\phi_{\boldsymbol{x}}^H,$$

where $S_{\mathcal{V}}$ is the set of subdomain vertices and $\boldsymbol{x}_0$, $\boldsymbol{x}_1$ are the endpoints of edge $\mathcal{E}$. When replacing I^H by $I^{\widetilde{H}}$, we have also that

$$\|I^{\widetilde{H}}(u-\widehat{u})\|^2_{L^\infty(\Omega_i)} \leq \|u-\widehat{u}\|^2_{L^\infty(\Omega_i)}.$$

Therefore, similar results as in Lemma 4.3 and Lemma 4.4 can be obtained. No new ideas are required to deduce a similar bound for the condition number of the preconditioned system as in Theorem 3.1. ∎

7. Experimental results. We present some numerical results for our two-level overlapping additive algorithm with $\Omega = [0,1]^2$. We consider meshes with triangular, square, hexagonal and irregular elements, with square subdomains (for triangular and square elements) and irregular subdomains (for all the types of elements) created with the mesh-partitioner software METIS [18]; for some examples see Figure 3 and Figure 4.

We solve the resulting linear systems using the preconditioned conjugate gradient method to a relative residual tolerance of 10^{-6}. We compute the right-hand side such that the exact solution is $u(x_1,x_2) = \sin(\pi x_1)\sin(\pi x_2)$ when $\rho = 1$. The number of iterations and condition number estimates (in parenthesis) are reported for each of the experiments.

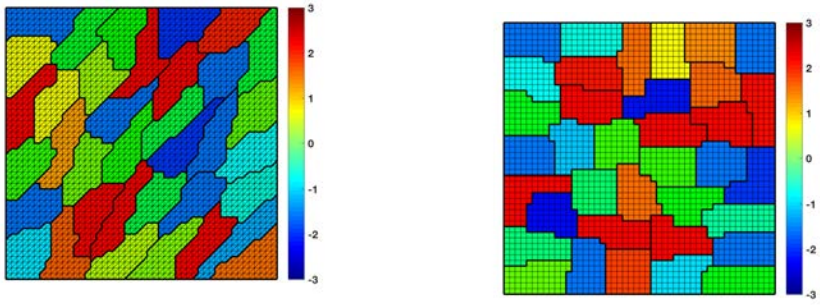

(a) Triangular elements and METIS subdomains

(b) Square elements and METIS subdomains

Fig. 3: Example of piecewise discontinuous ρ across the interface. For each subdomain, $\rho_i = 10^{r_i}$, where r_i is a random number in $[-3, 3]$ with a uniform distribution.

(a) Hexagonal elements and subdomains

(b) Irregular elements and subdomains

Fig. 4: Solution for $\rho = 1$ with virtual elements.

7.1. Standard Finite Element Spaces. We start by considering the discretization of problem (2) with the first-order Lagrange space P_1 (triangular elements) and the bilinear space Q_1 (square elements). In this case, our analysis provides a new coarse space for irregular subdomains. We note that our results are similar to the ones obtained in [10] where experiments were reported for a different coarse space based on discrete harmonic extensions, and that the dimension of our reduced coarse space is similar as theirs.

EXAMPLE 7.1. We verify the scalability of our algorithm. We first consider triangular elements with the first-order Lagrange space P_1 and square elements with the bilinear space Q_1, for a constant coefficient $\rho = 1$. We include experiments with square and METIS subdomains as in Figure 3. The condition number remains bounded as we increase the number of subdomains; see Table 1.

Table 1: Number of iterations and condition number (in parenthesis) for our algorithm discretized with P_1 and Q_1 elements with N subdomains, $\rho = 1$, $H/h = 16$ and $H/\delta = 4$. N_V is the dimension of the coarse space.

		Square subd		METIS subd		METIS reduc	
FEM	N	N_V	$I(\kappa)$	N_V	$I(\kappa)$	N_V	$I(\kappa)$
P_1	12^2	121	15(4.9)	1819	21(8.3)	243	26(9.9)
	16^2	225	15(4.8)	3308	26(10.6)	447	27(11.0)
	20^2	361	15(4.8)	5347	26(11.0)	711	29(13.5)
	24^2	529	15(4.7)	7651	30(10.8)	1054	27(10.8)
Q_1	12^2	121	14(5.5)	624	21(7.2)	241	22(7.7)
	16^2	225	14(5.9)	1265	24(7.3)	450	22(7.6)
	20^2	361	14(5.9)	2192	23(7.4)	721	22(7.2)
	24^2	529	14(5.7)	2685	23(7.4)	1058	22(7.0)

EXAMPLE 7.2. We confirm that the condition number grows linearly as a function of H/δ. In these experiments, we use 64 subdomains with $H/h = 64$, $\rho = 1$. The stiffness matrix has 263169 degrees of freedom. For square, METIS and reduced subdomains, the coarse space has dimension 49, 2923, 96 for P_1 elements, and 49, 1074 and 98 for Q_1 elements, respectively; see results in Figure 5.

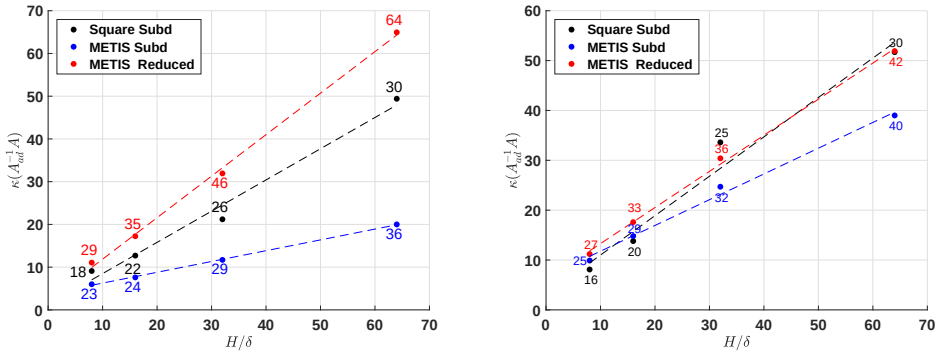

(a) Triangular elements

(b) Square elements

Fig. 5: Condition number ($y-$axis) as a function of H/δ (the number of iterations is shown for each point).

EXAMPLE 7.3. We study the behavior for increasing values of H/h with 64 subdomains, $H/\delta = 4$ and $\rho = 1$; see Table 2. Results in this case are insensitive to increasing values of H/h.

EXAMPLE 7.4. We study the behavior of our algorithm when ρ has discontinuities across the interface; see Figure 3 for a particular example of ρ. For each test we generate random numbers $r_i \in [-3, 3]$ with a uniform distribution, and assign $\rho_i = 10^{r_i}$ for individual elements inside each subdomain Ω_i. In this case, we observe the logarithmic factor $1 + \log(H/h)$ in some cases; see results in Table 3.

Table 2: Number of iterations and condition number (in parenthesis) for our algorithm discretized with P_1 and Q_1 elements with 64 subdomains, $\rho = 1$ and $H/\delta = 4$. N_V is the dimension of the coarse space and dof the size of the stiffness matrix.

			Square subd		METIS subd		METIS reduced	
FEM	H/h	dof	N_V	$I(\kappa)$	N_V	$I(\kappa)$	N_V	$I(\kappa)$
P_1	8	4225	49	14(5.2)	386	21(7.6)	93	25(10.2)
	16	16641	49	15(5.5)	386	22(7.9)	93	26(10.9)
	32	66049	49	16(5.7)	386	23(7.8)	93	27(10.8)
	64	263169	49	16(5.8)	386	23(7.8)	93	28(11.0)
Q_1	8	4225	49	14(6.0)	252	19(6.2)	96	19(5.7)
	16	16641	49	14(4.9)	252	20(6.3)	96	20(6.3)
	32	66049	49	15(4.8)	252	20(6.3)	96	21(6.4)
	64	263169	49	15(4.8)	252	21(6.4)	96	21(6.4)

Table 3: Number of iterations and condition number (in parenthesis) for our algorithm with P_1 and Q_1 elements and 64 subdomains, ρ discontinuous across the interface, $H/\delta = 4$.

		Square subd		METIS subd		METIS reduc	
FEM	H/h	N_V	$I(\kappa)$	N_V	$I(\kappa)$	N_V	$I(\kappa)$
P_1	16	49	25(11.6)	386	24(7.5)	93	26(8.7)
	32	49	27(14.0)	386	25(7.6)	93	27(8.8)
	64	49	27(16.3)	386	25(7.7)	93	27(8.8)
Q_1	16	49	25(17.6)	252	25(8.6)	96	24(7.4)
	32	49	26(20.6)	252	27(9.0)	96	26(9.3)
	64	49	27(23.6)	252	28(9.2)	96	27(9.7)

7.2. Discretizacion with VEM. We now consider general polygonal meshes as in Figure 4. We use our two-level additive algorithm in order to construct a preconditioner for the linear system that arises from (5); see [20] for a Matlab's implementation of the lowest-order VEM.

EXAMPLE 7.5. We first verify the scalability for $\rho = 1$; see Table 4 and Table 5. We add two layers of elements in order to construct Ω_i' in both cases and $H/h \approx 8$. For hexagonal and irregular elements we construct subdomains based on the incenter of the elements (to obtain square-like subdomains) and METIS subdomains. We observe that results agree with the bounds obtained in Theorem 3.1 and Theorem 6.1.

EXAMPLE 7.6. In this case, we study the behavior of the condition number for increasing values of H/δ for $\rho = 1$ and $H/h = 32$; see Figure 6. We observe linear growth as we increase H/δ, as expected.

EXAMPLE 7.7. We study the dependence on H/h for the different type of elements; see results in Table 6. We observe a logarithmic growth in the cases of hexagonal and irregular elements.

EXAMPLE 7.8. We conclude by presenting some examples where ρ has discontinuities across the interface as in Example 7.4. Results are independent of jumps of the coefficient across the interface; see Table 7 and Figure 7.

Table 4: Number of iterations and condition number (in parenthesis) for our algorithm with square elements and VEM. We add two layers of elements to construct the overlapping subdomains Ω_i'. N_V is the dimension of the coarse space, N the number of subdomains, $\rho = 1$ and $H/h = 8$.

	Square subd		METIS subd		METIS reduced	
N	N_V	$I(\kappa)$	N_V	$I(\kappa)$	N_V	$I(\kappa)$
12^2	121	13(6.7)	654	20(6.7)	243	21(6.8)
16^2	225	13(6.2)	1160	20(6.8)	439	21(7.1)
24^2	529	13(6.3)	2721	23(7.4)	1047	22(7.3)
32^2	961	12(5.4)	4711	24(7.6)	1891	22(7.5)

Table 5: Number of iterations and condition number (in parenthesis) for our reduced algorithm with hexagonal and irregular elements with VEM. We add two layers of elements to construct the overlapping subdomains Ω_i'. N_V is the dimension of the coarse space, N the number of subdomains, $\rho = 1$ and $H/h \approx 8$. The dimension of the reduced coarse represents only a 6% of the dimension of the full coarse space.

	Hexagonal elements				Irregular elements			
	Incenter		METIS		Incenter		METIS	
N	N_V	$I(\kappa)$	N_V	$I(\kappa)$	N_V	$I(\kappa)$	N_V	$I(\kappa)$
8^2	98	17(5.7)	99	17(5.0)	98	20(6.5)	99	23(7.7)
12^2	242	22(8.8)	242	24(8.6)	242	21(6.7)	247	24(10.5)
16^2	450	20(7.6)	453	22(7.8)	450	22(7.1)	452	24(8.1)
20^2	722	19(6.6)	721	22(7.1)	730	25(9.2)	724	25(8.7)

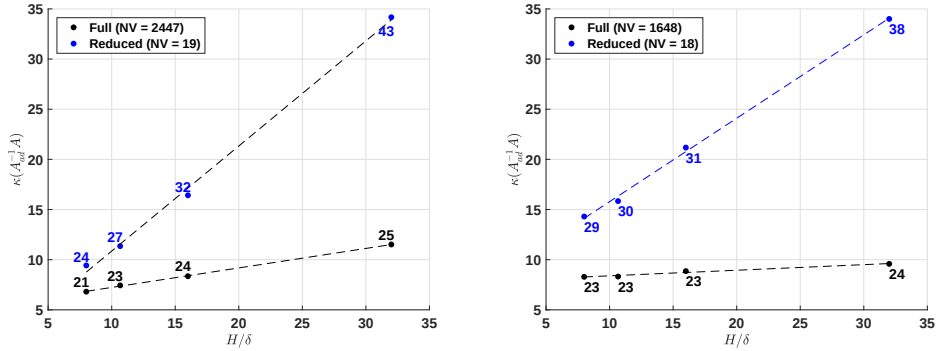

(a) Hexagonal elements

(b) Irregular elements

Fig. 6: Condition number ($y-$axis) as a function of H/δ for $\rho = 1$, $H/h = 32$, $N = 16$ (the number of iterations is shown for each point).

Table 6: Number of iterations and condition number (in parenthesis) for our reduced algorithm with 16 METIS subdomains, $\rho = 1$ and $H/\delta = 4$.

	Square elem		Hexagonal elem		Irregular elem	
H/h	N_V	$I(\kappa)$	N_V	$I(\kappa)$	N_V	$I(\kappa)$
16	17	19(6.1)	18	18(5.9)	18	22(7.4)
32	17	20(6.2)	18	19(6.1)	19	28(13.7)
64	17	20(6.2)	18	20(6.6)	18	37(20.9)

Table 7: Scalability for different VEM discretizations for the reduced coarse space with METIS subdomains, ρ discontinuous across the interface, $H/h = 8$, $H/\delta = 4$.

	Squares	Hexagons	Irregular
N	$I(\kappa)$	$I(\kappa)$	$I(\kappa)$
12^2	27(9.5)	28(10.2)	27(9.7)
16^2	26(9.1)	26(8.8)	29(10.2)
20^2	27(9.2)	26(8.0)	32(12.1)

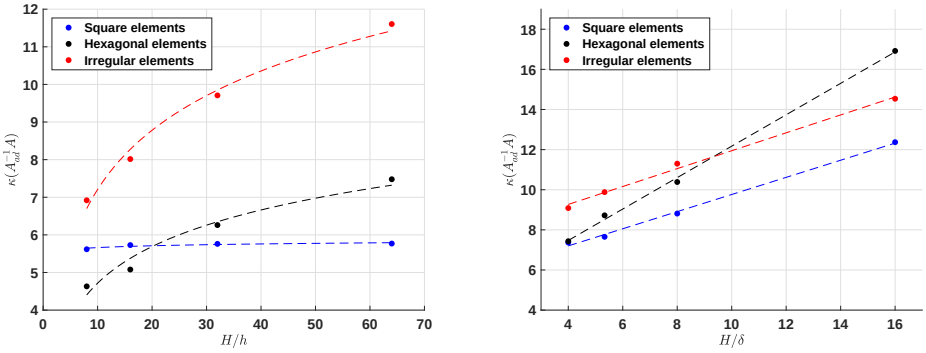

Fig. 7: Condition number as a function of H/h (left) and H/δ (right) for the reduced coarse space, with $N = 16$ and ρ discontinuous across the interface as in Figure 3.

8. Conclusions. We have defined a new coarse space V_0 that can be used for different domain decomposition methods which is useful in the presence of irregular subdomains. In particular, we have obtained a bound for the condition number of the preconditioned system by using a two-level overlapping Schwarz method, where we have used VEM for the discretization of problem (2). Nevertheless, the dimension of V_0 can grow if the edges are quite irregular, even for structured meshes. For that reason, we have introduced a reduced coarse space V_0^R. Its dimension is equal to the number of internal subdomain vertices and the estimates for the condition numbers are quite similar in both cases, even though there is a significant reduction in the dimension of the coarse space.

We have developed two sets of numerical experiments. First, the coarse spaces V_0 and V_0^R are used for standard P_1 and Q_1 discretizations; see Subsection 7.1. Our results are similar as the ones obtained in [10] where their coarse space is based on energy minimization. Second, we have tested the preconditioner for the stiffness matrix obtained by VEM, which allows to consider polygonal elements; see Subsection 7.2. In both cases, we have verified the theoretical bounds obtained in Theorem 3.1 and Theorem 6.1. Results are competitive and independent of jumps of the coefficient across the subdomains, and the method allows to handle irregular subdomains as the ones obtained by mesh partitioners.

Acknowledgments. The author would like to thank his former advisor Prof. Olof Widlund and Prof. Tomáš Vejchodský for their suggestions during the work on this article.

REFERENCES

[1] L. Beirão da Veiga, F. Brezzi, A. Cangiani, G. Manzini, L. D. Marini, and A. Russo, *Basic principles of virtual element methods*, Math. Models Methods Appl. Sci., 23 (2013), pp. 199–214.

[2] L. Beirão da Veiga, F. Brezzi, L. D. Marini, and A. Russo, *The hitchhiker's guide to the virtual element method*, Math. Models Methods Appl. Sci., 24 (2014), pp. 1541–1573.

[3] J. H. Bramble and S. R. Hilbert, *Estimation of linear functionals on Sobolev spaces with application to Fourier transforms and spline interpolation*, SIAM J. Numer. Anal., 7 (1970), pp. 112–124.

[4] S. Brenner and R. Scott, *The Mathematical Theory of Finite Element Methods*, Texts in Applied Mathematics, Springer New York, 2007.

[5] E. Cáceres, *Mixed Virtual Element Methods. Applications in Fluid Mechanics.*, 2015. Thesis (Ph.D.)–Universidad de Concepción, Chile.

[6] J. G. Calvo, *A two-level overlapping Schwarz method for H(curl) in two dimensions with irregular subdomains*, Electron. Trans. Numer. Anal., 44 (2015), pp. 497–521.

[7] ———, *A BDDC algorithm with deluxe scaling for $H(curl)$ in two dimensions with irregular subdomains*, Math. Comp., 85 (2016), pp. 1085–1111.

[8] C. R. Dohrmann, A. Klawonn, and O. B. Widlund, *Domain decomposition for less regular subdomains: Overlapping Schwarz in two dimensions*, SIAM J. Numer. Anal., 46 (2008), pp. 2153–2168.

[9] C. R. Dohrmann, A. Klawonn, and O. B. Widlund, *A family of energy minimizing coarse spaces for overlapping Schwarz preconditioners*, in Domain decomposition methods in science and engineering XVII, vol. 60 of Lect. Notes Comput. Sci. Eng., Springer, Berlin, 2008, pp. 247–254.

[10] C. R. Dohrmann and O. B. Widlund, *An alternative coarse space for irregular subdomains and an overlapping Schwarz algorithm for scalar elliptic problems in the plane*, SIAM J. Numer. Anal., 50 (2012), pp. 2522–2537.

[11] C. R. Dohrmann and O. B. Widlund, *An iterative substructuring algorithm for two-dimensional problems in $H(curl)$*, SIAM J. Numer. Anal., 50 (2012), pp. 1004–1028.

[12] C. R. Dohrmann and O. B. Widlund, *On the design of small coarse spaces for domain decomposition algorithms*, Tech. Rep. TR2017-987, Courant Institute, NYU, 2017.

[13] M. Dryja and O. B. Widlund, *An additive variant of the Schwarz alternating method for the case of many subregions*, Tech. Rep. TR-339, Department of Computer Science, Courant Institute, 1987.
[14] ———, *Some domain decomposition algorithms for elliptic problems*, in Iterative methods for large linear systems (Austin, TX, 1988), Academic Press, Boston, MA, 1990, pp. 273–291.
[15] ———, *Towards a unified theory of domain decomposition algorithms for elliptic problems*, in Third International Symposium on Domain Decomposition Methods for Partial Differential Equations (Houston, TX, 1989), SIAM, Philadelphia, PA, 1990, pp. 3–21.
[16] F. John, *Rotation and strain*, Comm. Pure Appl. Math., 14 (1961), pp. 391–413.
[17] P. W. Jones, *Quasiconformal mappings and extendability of functions in Sobolev spaces*, Acta Math., 147 (1981), pp. 71–88.
[18] G. Karypis and V. Kumar, *A fast and high quality multilevel scheme for partitioning irregular graphs*, SIAM J. Sci. Comput., 20 (1998), pp. 359–392.
[19] A. Klawonn, O. Rheinbach, and O. B. Widlund, *An analysis of a FETI-DP algorithm on irregular subdomains in the plane*, SIAM J. Numer. Anal., 46 (2008), pp. 2484–2504.
[20] O. J. Sutton, *The virtual element method in 50 lines of MATLAB*, Numerical Algorithms, (2016), pp. 1–19.
[21] A. Toselli and O. B. Widlund, *Domain decomposition methods-algorithms and theory*, vol. 34 of Springer Ser. Comput. Math., Springer, 2005.
[22] O. B. Widlund, *Accommodating irregular subdomains in domain decomposition theory*, in Domain Decomposition Methods in Science and Engineering XVIII, M. Bercovier, M. J. Gander, R. Kornhuber, and O. B. Widlund, eds., vol. 70 of Lecture Notes in Computational Science and Engineering, Springer-Verlag, 2009, pp. 87–98.